

## Thermal conductivity and interfacial resistance in single-wall carbon nanotube epoxy composites

M. B. Bryning,<sup>a)</sup> D. E. Milkie, M. F. Islam, J. M. Kikkawa, and A. G. Yodh  
*Department of Physics and Astronomy, University of Pennsylvania, 209 S. 33rd Street, Philadelphia, Pennsylvania 19104-6396*

(Received 13 June 2005; accepted 23 August 2005; published online 12 October 2005)

We report thermal conductivity measurements of *purified* single-wall carbon nanotube (SWNT) epoxy composites prepared using suspensions of SWNTs in N-N-Dimethylformamide (DMF) and surfactant stabilized aqueous SWNT suspensions. Thermal conductivity enhancement is observed in both types of composites. DMF-processed composites show an advantage at SWNT volume fractions between  $\phi \sim 0.001$  to 0.005. Surfactant processed samples, however, permit greater SWNT loading and exhibit larger overall enhancement ( $64 \pm 9\%$ ) at  $\phi \sim 0.1$ . The enhancement differences are attributed to a ten-fold larger SWNT/solid-composite interfacial thermal resistance in the surfactant-processed composites compared to DMF-processed composites. The interfacial resistance is extracted from the volume fraction dependence of the thermal conductivity data using effective medium theory. [C. W. Nan, G. Liu, Y. Lin, and M. Li, *Appl. Phys. Lett.* **85**, 3549 (2004)]. © 2005 American Institute of Physics. [DOI: 10.1063/1.2103398]

Single-wall carbon nanotubes (SWNTs) are rodlike macromolecules with a thermal conductivity possibly surpassing even that of diamond and multiwall carbon nanotubes.<sup>1-3</sup> Thus, there continues to be substantial interest in SWNTs as additives for enhancing the thermal conductivity of insulating materials. For instance, multifunctional materials that provide the physical strength and light weight of epoxy, combined with high thermal and/or electrical conductivity, would find numerous aerospace and semiconductor applications. The potential for such materials will depend on an improved understanding and control of many factors including thermal interfacial resistances arising between SWNTs and the surrounding matrix, and the quality and nature of the nanotube network.

Thermal conductivity enhancements due to inclusions of raw (unpurified) carbon nanotubes in epoxy,<sup>4</sup> silicon elastomer,<sup>5</sup> and oil<sup>6</sup> have been reported. The degree of enhancement in these studies at 1 wt % loading varies substantially [from  $\sim 15\%$  (Ref. 7) to  $\sim 160\%$  (Ref. 8)], perhaps as a result of nanotube type (single vs. multi-wall tubes), dispersion quality, nanotube purity and length, composite preparation, and thermal interfacial resistance,  $R_K$ . Indeed,  $R_K$  was found to be quite large in recent laser pump-probe measurements of dilute aqueous suspensions of sodium dodecyl sulfate surfactant stabilized SWNTs.<sup>7</sup> Theoretical models<sup>8-11</sup> for these thermal transport processes and related simulations<sup>12,13</sup> have also been developed.

We report on thermal conductivity measurements of *purified* SWNT in epoxy composites in a comparative study of two practical starting formulations. Both achieve fairly homogeneous SWNT distributions within an epoxy matrix using either surfactant stabilized aqueous SWNT suspensions (surfactant processed) or metastable SWNT / N-N-Dimethylformamide (DMF) suspensions (DMF processed). To our knowledge, this is the first thermal conductivity study of SWNT composites to use highly purified SWNTs. Raw SWNT material often contains significant carbonaceous and

metallic impurities on SWNT surfaces and in the bulk, which can adversely affect composite performance and complicate quantitative analysis of composite properties. The conductivity enhancements are ( $27 \pm 5\%$ ) in the DMF-processed composites at SWNT volume fractions  $\phi \sim 0.005$ , and ( $64 \pm 9\%$ ) in the surfactant processed samples at  $\phi \sim 0.1$ . Analytical fits of effective medium theory to our measurements provide first estimates of SWNT interfacial resistance in solid composites, and demonstrate a ten-fold larger  $R_K$  in surfactant-processed samples compared to DMF-processed samples. The increase in  $R_K$  may be attributed to a surfactant layer coating the SWNTs.

SWNTs produced by the high pressure decomposition of carbon monoxide (HiPco) method (Carbon Nanotechnologies, Inc., Batch 79) are obtained in raw form and are purified as described in Ref. 14. The purified material contains  $>90$  wt% SWNTs,  $<5$  wt% carbon derivative, and  $\leq 0.96$  wt% magnetic catalyst.<sup>15,16</sup> The electrical properties of the purified SWNTs are not significantly affected by purification.<sup>14</sup> Atomic force microscopy (AFM) measurements of the SWNT dimensions give a mean length of  $L = 167 \pm 90$  nm and a mean diameter of  $d = 1.1 \pm 0.3$  nm.<sup>17</sup> Longer laser-oven SWNTs ( $L = 516 \pm 286$  nm,  $d = 1.35 \pm 0.15$  nm)<sup>17</sup> also used in this study are purified and processed in a similar way.<sup>18</sup>

Both DMF- and surfactant-processed samples are prepared with identical procedures, differing only in the initial SWNT suspension. DMF-processed samples use a very dilute (0.0004 wt %) suspension of SWNTs in DMF.<sup>16</sup> Surfactant-processed samples use a dilute (0.005 wt %) aqueous suspension of sodium dodecylbenzene sulfonate (NaDDBS) surfactant stabilized SWNTs.<sup>17</sup> The weight ratio of NaDDBS to SWNTs in these suspensions is 1:1. The starting suspension is added to the epoxy resin (Miller Stephenson Epon 828) and the solvent is allowed to evaporate prior to crosslinking (Miller Stephenson EpiKure 3234). Details of the process and electrical conductivity measurements for the DMF-processed samples are reported in Ref. 16. In DMF processing the resin becomes highly viscous at  $\phi > 0.005$ ,

<sup>a)</sup>Electronic mail: mbryning@physics.upenn.edu

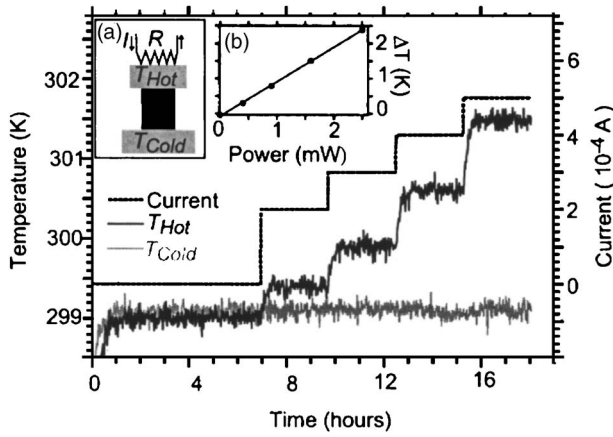


FIG. 1. Inset (a) depicts the measurement setup. The main plot shows the applied current and corresponding temperature response of the top and bottom plates. In inset (b), the slope of the applied power ( $I^2R$ ) vs the temperature differential ( $\Delta T$ ) gives the thermal conductance of the sample, from which thermal conductivity is extracted.

while in surfactant-processing SWNT volume fractions as high as  $\phi=0.1$  are possible. This difference may be attributed to the longer gelation time of the surfactant stabilized samples,<sup>19</sup> but both types of processing produced homogeneous dispersions of SWNTs in the matrix, down to a length scale of a few  $\mu\text{m}$ . The SWNT volume fraction,  $\phi$ , was determined by using the calculated value for SWNT density of  $1.4\text{ g/cm}^3$  (Ref. 20) and the measured density of cured pure epoxy (Ref. 16) ( $1.2\pm 0.02\text{ g/cm}^3$ ).

Thermal conductivity measurements follow the “two thermometer-one heater” method using a custom-built stage designed for the Quantum Design Physical Property Measurement System (PPMS). Cernox thermometers (LakeShore Cryotronics, Inc.) monitor the temperature of two polished oxygen-free high-conductivity (OFHC) copper plates contacted to the ends of a cylindrical ( $\sim 5.3\text{ mm}$  height  $\times$   $\sim 4.7\text{ mm}$  diameter) sample. A  $10\text{ k}\Omega$  surface mount resistor heats the top plate ( $10\text{ mm}$  diameter  $\times$   $1\text{ mm}$  thick) to a temperature  $T_{\text{Hot}}$ . Heat flows from the top plate, through the sample, and into the bottom plate which is thermally grounded to  $T_{\text{Cold}}$  by the PPMS. Apiezon N-grease enhances thermal contact to the sample.<sup>21</sup> A gold-plated radiation cap around the stage fixed at  $T_{\text{Cold}}$  and a high vacuum ( $<10^{-5}$  Torr) reduce thermal losses due to radiation and convection, respectively.

A typical measurement (see Fig. 1) consists of incrementing the heater current in four to five steps. Temperature differentials ( $\Delta T = T_{\text{Hot}} - T_{\text{Cold}}$ ) of  $\sim 0.2$  to  $2.5\text{ K}$  are allowed to stabilize between each step for  $\sim 3\text{ h}$ , and thermal conductivity,  $\kappa$ , is extracted from the slope of applied power  $I^2R$  versus  $\Delta T$  according to

$$I^2R = (\kappa\pi r^2/L + K_{\text{Loss}})\Delta T + P_{\text{Rad}}, \quad (1)$$

where  $r$  and  $L$  are the cylindrical radius and length, respectively, and  $K_{\text{Loss}}\Delta T$  is the total heat loss through the manganin electrical leads and residual gas.

The heat loss due to radiation,  $P_{\text{Rad}}$ , is estimated by the Stefan-Boltzmann law,

$$P_{\text{Rad}} = (\epsilon_1\epsilon_2/(\epsilon_1 + \epsilon_2 - \epsilon_1\epsilon_2))\sigma A_H(T_{\text{Hot}}^4 - T_{\text{Cold}}^4). \quad (2)$$

Here,  $\epsilon_1$  and  $\epsilon_2$  are the emissivities of the hot and cold surfaces,  $\sigma$  is the Stefan-Boltzmann constant, and  $A_H$  is the area

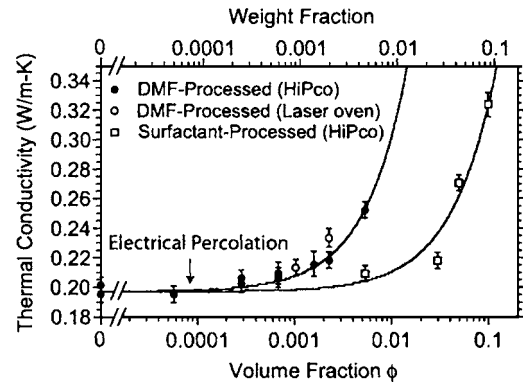


FIG. 2. Thermal conductivity of DMF-processed and surfactant-processed samples. The fits shown assume SWNT dimensions ( $L=167\text{ nm}$ ,  $d=1.1\text{ nm}$ ), thermal conductivities of SWNTs ( $\kappa_{\text{SWNT}}=3000\text{ W/m-K}$ ), and epoxy ( $\kappa_m=0.198\text{ W/m-K}$ ). The thermal interface resistance ( $R_K$ ) is the free fit parameter.  $\phi$  is known to within  $\pm 10\%$ .

of the hot surface. This formulation is valid for reflecting concentric cylinders and parallel planes.<sup>22</sup> The maximum calculated radiative loss (at  $\Delta T=2.5\text{ K}$ ) from the heated top plate, given  $A_H=2\times 10^{-4}\text{ m}^2$  and  $\epsilon_1=\epsilon_2=0.05$  for polished metal,<sup>23</sup> is  $\sim 3\%$  of the applied power. Additional radiative losses also occur from the temperature gradient in the sample itself. Assuming a worst-case  $\epsilon=1$  for the samples, the maximum radiative loss from the sample surface is  $\sim 1.2\%$  of the applied power.  $K_{\text{Loss}}$  was estimated by measuring a styrofoam cylinder and a hollow polystyrene straw with geometries nearly identical to the composite samples. The experiments clearly indicated that  $K_{\text{Loss}} \gg \kappa\pi r^2/L$  for these insulators, and  $K_{\text{Loss}}$  was determined to be  $(4.18\pm 0.09)\times 10^{-4}\text{ W/K}$ .

The measured thermal conductivities are shown in Fig. 2. DMF-processed samples exhibit a modest enhancement of  $\kappa$  in the range  $\phi\approx 0.001$  to  $0.005$ . At  $\phi=0.005$ , the enhancement is about  $(27\pm 5)\%$  over pure epoxy. In contrast, surfactant-processed composites exhibit no measurable enhancement below  $\phi\approx 0.01$ , and  $(64\pm 9)\%$  at  $\phi=0.1$ . The electrical conductivity of DMF-processed composites undergoes a discontinuous change of about five orders of magnitude<sup>16</sup> near the threshold volume fraction of  $\sim 1\times 10^{-4}$ , but no such discontinuity is observed in the thermal conductivity. Thus, electrical percolation has no significant effect on the thermal conductivity enhancement, consistent with a phonon-dominated picture of SWNT thermal transport. Effective medium theory is suitable when percolation effects can be neglected, and enables estimation of the interfacial resistance  $R_K$  at the SWNT/matrix interface.

A formulation of effective medium theory appropriate to the present case<sup>24</sup> considers a system of randomly oriented rods in a host medium.<sup>8</sup> The effective thermal conductivity of the composite is

$$\kappa_{\text{eff}} = \kappa_m \frac{(3 + \phi(\beta_{\perp} + \beta_{\parallel}))}{(3 - \phi\beta_{\perp})}, \quad (3)$$

where

$$\beta_{\perp} = \frac{2(d(\kappa_{\text{SWNT}} - \kappa_m) - 2R_K\kappa_{\text{SWNT}}\kappa_m)}{d(\kappa_{\text{SWNT}} + \kappa_m) + 2R_K\kappa_{\text{SWNT}}\kappa_m}, \quad (4a)$$

TABLE I. Table of thermal conductivity enhancements and calculated interfacial resistances. Enhancements are quoted for 1 wt % nanotube loadings, except for Ref. 6, which is quoted for 1 vol % SWNT.

Composite type	Enhancement	$R_K(\text{m}^2\text{K}/\text{W})$
SWNT / epoxy (DMF)	80% (fit)	$(2.4 \pm 1.3) \times 10^{-9}$
SWNT / epoxy (Surf.)	<8%	$(2.6 \pm 0.9) \times 10^{-8}$
SWNT / epoxy <sup>a</sup>	125%	...
Multiwall nanotube (MWNT) / silicone <sup>b</sup>	~15%	...
MWNT / oil <sup>c</sup>	160%	$8 \times 10^{-8}$ <sup>e</sup>
SWNT / water <sup>d</sup>	...	$8.3 \times 10^{-8}$

<sup>a</sup>See Ref. 4.

<sup>b</sup>See Ref. 5.

<sup>c</sup>See Ref. 6.

<sup>d</sup>See Ref. 7.

<sup>e</sup>See Ref. 8.

$$\beta_{\parallel} = \frac{L(\kappa_{\text{SWNT}} - \kappa_m) - 2R_K\kappa_{\text{SWNT}}\kappa_m}{L\kappa_m + 2R_K\kappa_{\text{SWNT}}\kappa_m}, \quad (4b)$$

and the thermal conductivities of the epoxy and SWNTs are  $\kappa_m$  and  $\kappa_{\text{SWNT}}$ , respectively. Our measurements of pure epoxy give  $\kappa_m = 0.198 \pm 0.005$  W/m-K. Published measurements and simulations bound  $\kappa_{\text{SWNT}}$  between (Ref. 4) 1750 W/m-K and (Ref. 3) 6600 W/m-K. We use a value of 3000 W/m-K for fitting. AFM measurements of HiPco SWNTs give mean length  $L = 167$  nm and mean diameter  $d = 1.1$  nm. Given these parameters, we obtain fits to our data, as shown in Fig. 2, with  $R_K = (2.4 \pm 1.3) \times 10^{-9}$  m<sup>2</sup>K/W for DMF-processed samples and  $R_K = (2.6 \pm 0.9) \times 10^{-8}$  m<sup>2</sup>K/W for surfactant-processed samples. The enhancement predicted at 1 wt % SWNTs ( $\phi = 0.012$ ) for DMF processed composites is 80%, compared to 125% obtained in earlier studies of similar SWNT epoxy composites.<sup>4</sup> The difference may be attributed to several factors, including the lower aspect ratio of HiPco SWNTs compared to laser-oven SWNTs (Ref. 17) used in the previous study and the differences between raw and purified starting dispersions. Limited measurements of laser-oven SWNT DMF-processed composites (see Fig. 2) appear in the same range as the HiPco data. Table I compares our results to other studies.

The difference in the interfacial resistance between the DMF-processed and surfactant-processed samples is attributed to the surfactant, which coats the SWNTs and reduces heat transfer. The value for  $R_K$  obtained by laser pump-probe measurements for SDS surfactant stabilized aqueous SWNT suspensions was  $R_K = 8.3 \times 10^{-8}$  m<sup>2</sup>K/W,<sup>7</sup> comparable to our surfactant-processed solid-epoxy results. Clearly, interfacial resistance limits the utility of SWNTs for enhancing thermal properties of insulating materials. Comparative measure-

ments of this parameter, such as those presented here, can elucidate contributing factors and ultimately lead to materials with reduced interfacial resistance and higher composite thermal conductivity.

The authors gratefully acknowledge useful discussions about SWNT composites with A. T. Johnson Jr. and K. I. Winey. This work is supported by grants from the NSF [No. MRSEC DMR-0079909 (for authors A.G.Y., J.M.K.), and DMR-0203378 (for A.G.Y.)], IGERT [No. DGE-0221664 (for author D.E.M.)], SENS (for author D.E.M.), NASA [No. NAG8-2172 (for author A.G.Y.)], and DARPA/ONR [No. N00015-01-1-0831 (for author J.M.K.)].

<sup>1</sup>J. Hone, B. Batlogg, Z. Benes, A. T. Johnson, and J. E. Fischer, *Science* **289**, 1730 (2000).

<sup>2</sup>S. Berber, Y.-K. Kwon, and D. Tománek, *Phys. Rev. Lett.* **84**, 4613 (2000).

<sup>3</sup>J. Hone, M. Whitney, C. Piskoti, and A. Zettl, *Phys. Rev. B* **59**, R2514 (1999).

<sup>4</sup>M. J. Biercuk, M. C. Llaguno, M. Radosavljevic, J. K. Hyun, A. T. Johnson, and J. E. Fischer, *Appl. Phys. Lett.* **80**, 2767 (2002).

<sup>5</sup>C. H. Liu, H. Huang, Y. Wu, and S. S. Fan, *Appl. Phys. Lett.* **84**, 4248 (2004).

<sup>6</sup>S. U. S. Choi, Z. G. Zhang, W. Yu, F. E. Lockwood, and E. A. Grulke, *Appl. Phys. Lett.* **79**, 2252 (2001).

<sup>7</sup>S. T. Huxtable, D. G. Cahill, S. Shenogin, L. Xue, R. Ozisik, P. Barone, M. Usrey, M. S. Strano, G. Siddons, M. Shim, and P. Keblinski, *Nat. Mater.* **2**, 731 (2003).

<sup>8</sup>C. W. Nan, G. Liu, Y. Lin, and M. Li, *Appl. Phys. Lett.* **85**, 3549 (2004).

<sup>9</sup>C. W. Nan, Z. Shi, and Y. Lin, *Chem. Phys. Lett.* **375**, 666 (2003).

<sup>10</sup>C. W. Nan, R. Birringer, D. R. Clarke, and H. Gleiter, *J. Appl. Phys.* **81**, 6692 (1997).

<sup>11</sup>T. Chen, G. J. Weng, and W. C. Liu, *J. Appl. Phys.* **97**, 104312 (2005).

<sup>12</sup>M. Foygel, R. D. Morris, D. Anez, S. French, and V. L. Sobolev, *Phys. Rev. B* **71**, 104201 (2005).

<sup>13</sup>S. Shenogin, L. Xue, R. Ozisik, P. Keblinski, and D. G. Cahill, *J. Appl. Phys.* **95**, 8136 (2004)

<sup>14</sup>D. E. Johnston, M. F. Islam, A. G. Yodh, and A. T. Johnson, *Nat. Mater.* **4**, 589 (2005).

<sup>15</sup>M. F. Islam, D. E. Milkie, C. L. Kane, A. G. Yodh, and J. M. Kikkawa, *Phys. Rev. Lett.* **93**, 037404 (2004).

<sup>16</sup>M. B. Bryning, M. F. Islam, J. M. Kikkawa, and A. G. Yodh, *Adv. Mater. (Weinheim, Ger.)* **17**, 1186 (2005).

<sup>17</sup>M. F. Islam, E. Rojas, D. M. Bergey, A. T. Johnson, and A. G. Yodh, *Nano Lett.* **3**, 269 (2003).

<sup>18</sup>M. F. Islam, D. E. Milkie, O. N. Torrens, A. G. Yodh, and J. M. Kikkawa, *Phys. Rev. B* **71**, 201401 (2005).

<sup>19</sup>L. A. Hough, M. F. Islam, P. A. Janmey, and A. G. Yodh, *Phys. Rev. Lett.* **93**, 168102 (2004).

<sup>20</sup>G. Gao, T. Çağın, and W. A. Goddard III, *Nanotechnology* **9**, 184 (1998).

<sup>21</sup>E. Gmelin, M. Asen-Palmer, M. Reuther, and R. Villar, *J. Phys. D* **32**, R19 (1999).

<sup>22</sup>O. A. Saunders, *Proc. Phys. Soc. London* **41**, 569 (1928).

<sup>23</sup>F. Pobell, *Matter and Methods at Low Temperatures*, 2nd ed. (Springer, Berlin, 1996).

<sup>24</sup>That is, with approximations that are better suited for long, thin, and randomly oriented conducting rods.